

Model Peptides Uncover the Role of the β -Secretase Transmembrane Sequence in Metal Ion Mediated Oligomerization

Lisa M. Munter,^{†,‡} Holger Sieg,[‡] Tobias Bethge,^{‡,∇} Filip Liebsch,^{†,#} Frank S. Bierkandt,[§] Michael Schlegler,^{||,○} Heiko J. Bittner,[⊥] Joachim Heberle,^{||} Norbert Jakubowski,[§] Peter W. Hildebrand,[⊥] and Gerd Multhaup^{*,†,‡}

[†]Department of Pharmacology and Therapeutics, McGill University, 3655 Promenade Sir William Osler, H3G 1Y6 Montreal, Canada

[‡]Institut für Chemie und Biochemie, Freie Universität Berlin, Thielallee 63, 14195 Berlin, Germany

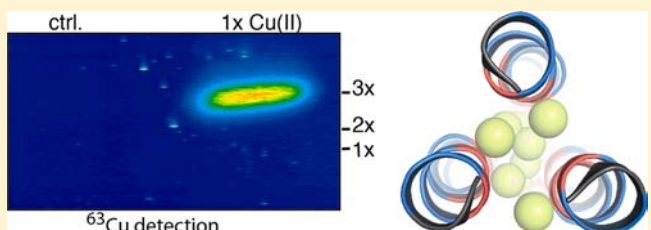
[§]Division 1.1 "Inorganic Trace Analysis", BAM Federal Institute for Materials Research and Testing, Richard-Willstätter-Straße 11, 12489 Berlin, Germany

^{||}Experimental Molecular Biophysics, Freie Universität Berlin, Arnimallee 14, 14195 Berlin, Germany

[⊥]Institut für Medizinische Physik und Biophysik, ProteInformatics Group, Charité, Charitéplatz 1, 10117 Berlin, Germany

Supporting Information

ABSTRACT: The β -secretase or β -site amyloid precursor protein cleaving enzyme 1 (BACE1) is the enzyme responsible for the formation of amyloid- β peptides, which have a major role in Alzheimer pathogenesis. BACE1 has a transmembrane sequence (TMS), which makes it unique among related proteases. We noticed that the BACE1 TMS contains an uncommon sulfur-rich motif. The sequence MxxxCxxxMxxxCxMxC spans the entire TMS, resembles metal ion binding motifs, and is highly conserved among homologues. We used a synthetic 31-mer model peptide comprising the TMS to study metal ion binding and oligomerization. Applying diverse biochemical and biophysical techniques, we detected dimer and trimer formation of the TMS peptide with copper ions. Replacement of the central Cys466 by Ala essentially abolished these effects. We show that the peptide undergoes a redox reaction with copper ions resulting in a disulfide bridge involving Cys466. Further, we find peptide trimerization that depends on the presence of monovalent copper ions and the sulfhydryl group of Cys466. We identified Cys466 as a key residue for metal ion chelation and to be the core of an oligomerization motif of the BACE1-TMS peptide. Our results demonstrate a novel metal ion controlled oligomerization of the BACE1 TMS, which could have an enormous therapeutic importance against Alzheimer disease.



The figure consists of two parts. On the left is a fluorescence detection image labeled '63Cu detection' showing a bright spot in the '1x Cu(II)' condition compared to the 'ctrl.' condition. On the right is a 3D ribbon diagram of the BACE1 TMS peptide structure, showing a complex fold with several alpha-helices and beta-strands.

INTRODUCTION

The β -site amyloid precursor protein cleaving enzyme 1 (BACE1) is an aspartic acid protease and regulates a range of neuronal functions and the formation of myelin sheaths in peripheral nerve cell.^{1–4} BACE1 is best known for its role in shedding the amyloid precursor protein (APP). The enzyme catalyzes the first step in the production of the amyloid- β ($A\beta$) peptide which is considered causative of Alzheimer disease (AD).^{5,6} Human genetic studies provide growing evidence of a central role for BACE1 in the pathogenesis of AD, since mutations were discovered at the BACE1 cleavage site of APP that promote or decrease BACE1 cleavage efficiency and $A\beta$ formation.^{7,8}

The BACE1 ectodomain dimerizes and the BACE1 dimer mediates cellular cleavage of APP.^{9–11} BACE1 is a membrane-bound protease and possesses a characteristic transmembrane sequence (TMS).⁶ The BACE1 TMS is essential for its cellular localization, e.g., to retain BACE1 in the Golgi apparatus.¹² Both the TMSs, of BACE1 and of the substrate APP, are necessary for effective cleavage of APP.¹² BACE1 lacking the

TMS compromises APP cleavage.¹³ Thus, the TMS of BACE1 has an indispensable role for enzymatic activity, which is regulated by the lipid environment, especially by cerebroside, anionic glycerophospholipids, and sterols.¹⁴ The TMS determines the activity and has been discovered as an important target for BACE1 regulation. First, a membrane-anchored inhibitor blocked β -secretase more efficiently than the free inhibitor in cultured cells did.¹⁵ Likewise, a noncompetitive inhibitor (TAK-070) was only active when it bound to the membrane-spanning sequence.¹⁶ Further, it was found that the mammalian CutA copper binding protein (the *E. coli* CutA divalent cation tolerance homologue) interacts with the TMS of BACE1 and regulates APP shedding through a reduction of the steady-state level of cell surface BACE1.¹⁷

We observed that the BACE1 TMS sequence is also unique for harboring a highly conserved sulfur-rich motif (MxxxCxxxMxxxCxMxC) which resembles binding sites for

Received: October 24, 2013

Published: December 4, 2013

copper (Cu) ions of Cu-transporting proteins like Sco1 (CxxxC) or Ctrl1 (MxxxM).^{18–20} Cu is an essential trace element and required for many physiological functions.²¹ An imbalance in cerebral Cu homeostasis is associated with the pathogenesis of AD.^{22–26} Multiple putative links between BACE1 and Cu metabolism are given by the findings that BACE1 as well as its substrates APP and A β bind Cu ions.^{27–30} Particularly, the cytoplasmic domain of BACE1 is known to bind a single Cu(I) ion with high affinity through conserved amino acid residues.³¹ Also, the intracellular Cu transporter CCS (copper chaperone of Cu/Zn-superoxide dismutase SOD1), which delivers Cu specifically to SOD1, directly binds to the BACE1 cytoplasmic domain.^{31,32}

In the present study we investigated whether the sulfur-rich core motif MxxxCxxxM is involved in metal ion coordination and oligomerization. Addition of Cu(II) facilitated the formation of dimers and trimers of a synthetic 31-amino acid peptide covering the BACE1 TMS. Importantly, we observed that the dimer is oxidized and loses its ability to bind metal ions, whereas peptides retaining their SH-groups form trimeric complexes containing monovalent Cu(I) or Ag(I). Using a bioinformatics approach that predicts TMS interactions from the sequence, we identified a recurrent TMS oligomerization motif centered around Cys466. Our results propose that BACE1 might play a role in Cu ion transport or in sensing of Cu ion concentrations.

RESULTS

Sulfur-Rich BACE1 TMS. The TMSs of BACE1 orthologues show that the TMSs of human (*Homo sapiens*, H.s.), mouse (*Mus musculus*, M.m.), rat (*Rattus norvegicus*, R.n.), cattle (*Bos taurus*, B.t.), and guinea pig (*Cavia porcellus*, C.p.) are conserved and revealed the existence of a Met- and Cys-rich sequence (M₄₆₂xxxC₄₆₆xxxM₄₇₀xxxM₄₇₄xM₄₇₆xM₄₇₈) spanning almost the entire TMS from position 462 to 478 of BACE1 (Figure 1a). Five out of the six sulfur-containing residues were found to be identical between all species, even in distantly related species such as zebra fish (*Danio rerio*, D.r.), claw frog (*Xenopus tropicalis*, X.t.), and green-spotted puffer fish (*Tetraodon nigroviridis*, T.n.) (Figure 1a). The six sulfur-containing residues in mammals reach a proportion of 30% of the TMS, which is about five times more than statistically expected compared to other known transmembrane helices (4.6% for Met and 1.2% for Cys³³ = 5.8%). Thus, model peptides encompassing the human BACE1 TMS (see Methods section) were designed to investigate this sulfur-rich core motif M₄₆₂xxxC₄₆₆xxxM₄₇₀ and named BACE1-TMS in the following.

Cu-Induced Oligomerization of the Peptide BACE1-TMS. The model peptide BACE1-TMS possesses more than 50% hydrophobic residues and was soluble in 80% methanol. For SDS-PAGE analysis, the BACE1-TMS peptide was incubated with CuCl₂ at the molar ratios indicated (Figure 1b). The gel shows a concentration-dependent formation of BACE1-TMS peptide dimers and trimers. Trimers were most prominent at subequimolar and equimolar ratios of peptide:Cu(II) (0.25x–1x). However, a several-fold molar excess of Cu(II) mainly yielded dimers (10x–50x). Thus, the Cu(II)-dependent dynamics of oligomerization suggests a direct interaction of Cu ions with the peptide. Importantly, the substitution variant peptide C466A of BACE1-TMS lacking the central Cys residue failed to show a Cu-induced oligomerization (Figure 1c).

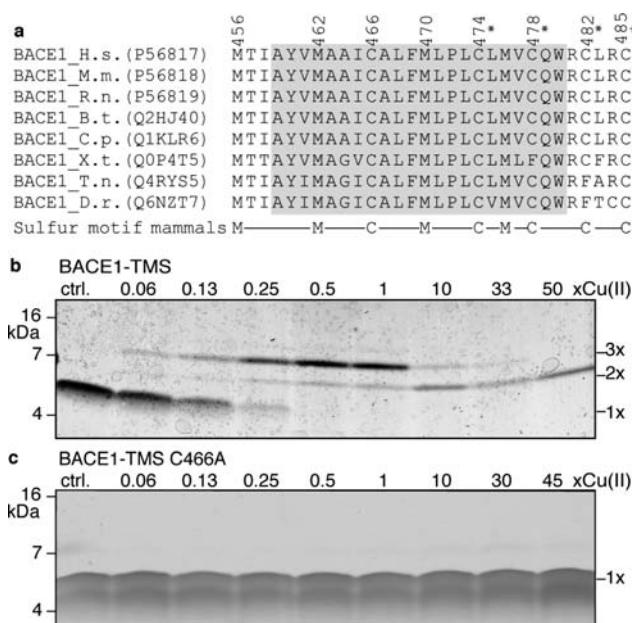


Figure 1. BACE1-TMS oligomerizes upon Cu ion treatment. (a) ClustalW2 alignment of the TMSs of BACE1 orthologs. Putative begin and end of TMS (gray box). Asterisks indicate potential palmitoylation. Numbering refers to H.s. UniProtKB reference numbers in brackets. (b) The BACE1-TMS peptide was incubated with CuCl₂ at molar ratios indicated (*x*-fold molar Cu(II)). (c) As (b) but variant peptide C466A. (b,c) Nonreducing conditions, silver-stained SDS-PA gel (*n* = 3).

Metal Ion Binding Analysis of the Peptide BACE1-TMS. To analyze if Cu ions directly bind to the peptide dimers and trimers, we used laser ablation inductively coupled plasma mass spectrometry (ICP-MS) to detect ⁶³Cu and ¹³C on the surface layer of a gel. One half of the gel was immediately stained with Coomassie brilliant blue as a positive control (Figure 2b), and the other half was rinsed in glycerol to withdraw water from the gel matrix before laser ablation ICP-MS analysis. The results are displayed as heat map elemental images (Figures 2a and S1). To normalize the quantity of detected copper to the equivalent sample size of the ablated gel matrix, the ⁶³Cu signals were calculated as the ratio of ⁶³Cu to ¹³C measures (Figure 2a). Ablated gels were subsequently stained with Coomassie brilliant blue to verify and match the peptide bands with the elemental images of the ablation (Figure S1d).

Figure 2a shows that the copper signal is exclusively associated with the trimeric peptide band, as indicated by the high ion intensity for ⁶³Cu in the surface plot. By contrast, no band was present at the dimer position. Conclusively, Cu was bound exclusively by the trimers but not by the dimers. To minimize the possible loss of Cu weakly bound to the dimer during gel electrophoresis or following acidic fixation, gels were run under gentle conditions (20 mA) and not fixed before laser ablation ICP-MS analysis.

FT-IR Analysis and Raman Spectroscopy of the BACE1-TMS Peptide. Since we identified Cys466 as a key residue for Cu(II) mediated oligomerization of the peptide BACE1-TMS, we applied attenuated total reflection Fourier transform infrared (ATR/FT-IR) spectroscopy to investigate if selective oxidation of the SH group occurs when Cu(II) is added. Therefore, ATR/FT-IR absorption spectra of a rehydrated BACE1-TMS peptide film were recorded in the

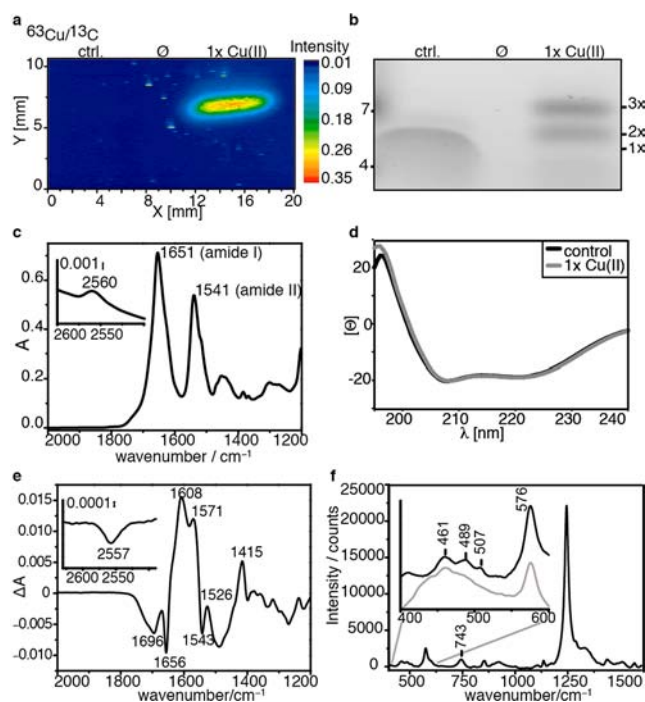


Figure 2. Dissection of dimer and trimer formation. (a) Laser ablation ICP-MS. (b) Coomassie brilliant blue stained gel, nonreducing conditions. (c) ATR/FT-IR absorbance spectra of the rehydrated peptide film. The S–H stretching vibration can be detected at 2560 cm^{-1} with an amplitude of $A = 1.2 \times 10^{-3}$. (d) CD spectroscopy of the BACE1-TMS peptide. Ellipticity in $10^3\text{ deg cm}^2\text{ dmol}^{-1}\text{ residue}^{-1}$. (e) IR difference spectra after addition of Cu(II). The negative difference band at 2557 cm^{-1} indicates disappearance of S–H stretching vibrations. (f) RAMAN spectra of the peptide film before (gray) and after Cu(II) addition (black). The vibrations at 489 and 507 cm^{-1} appear upon Cu(II) treatment.

mid-infrared region in the absence of Cu(II) (Figure 2c). The inset depicts the enlarged spectral region between 2600 and 2500 cm^{-1} with an absorption band at 2560 cm^{-1} characteristic for the thiol S–H stretching vibration.³⁴ The position of the absorption bands of the peptide bonds at 1651 cm^{-1} (predominantly C=O stretch, amide I) and 1541 cm^{-1} (C=N stretch coupled to N–H bending vibration, amide II) indicates a predominant α -helical secondary structure of the peptide. The α -helical structure of the peptide was also corroborated by circular dichroism (CD) spectroscopy in solution (Figure 2d). The conformation is retained even at equimolar concentrations of Cu(II) added, i.e., conditions where the trimer formation is strongly promoted.

For ATR/FT-IR measurements, a molar excess of Cu(II) was added to the peptide film, and the difference spectrum between the two states of the peptide in the presence and absence of Cu(II) was recorded (Figure 2e). The spectral window between 2600 and 2500 cm^{-1} , highlighted as inset, depicts a single negative difference band, which corresponds to the disappearance of the sulfhydryl stretching vibration of the Cys residue upon treatment with Cu(II).³⁴ The amplitude of $\Delta A = 4 \times 10^{-4}$ indicates the depletion of the thiol band by one-third of the corresponding band amplitude in the absorption spectrum ($A = 1.2 \times 10^{-3}$). Thus, the presence of Cu(II) induced a significant attenuation of the sulfhydryl vibration, most likely by oxidation of the SH groups and the intimately linked disulfide bridge formation. Also, the appearance of

negative difference bands at 1656 cm^{-1} (–, amide I) and 1543 cm^{-1} (–, amide II) indicate a slightly decreasing α -helical content in the secondary structure of the peptide ($\sim 1\%$) after addition of excess Cu(II).³⁵

Raman spectroscopy was performed to provide additional evidence of newly formed disulfide bonds (Figure 2f). The Raman spectrum recorded in the presence of Cu(II) (see spectral cutoff from 400 to 600 cm^{-1} , black line) showed two bands at 489 and 507 cm^{-1} which are at positions typical for S–S bonds but which are absent prior to the addition of Cu(II) (gray line). Thus, a new Raman active S–S stretching vibration was detected.³⁶ A Raman band at 743 cm^{-1} is also evident, which can be assigned to the C–S stretching vibration of the cysteine amino acid. Taken together, vibrational analyses by IR and Raman spectroscopies strongly imply the oxidation of Cys466 of BACE1-TMS induced by Cu ions. These results provide detailed support to our hypothesis of the concomitant formation of the intermolecular disulfide bond leading to BACE1-TMS dimerization. However, the dimer is unable to bind Cu ions as indicated by laser ablation ICP-MS.

Involvement of Monovalent Transition-Metal Ions in Oligomer formation. The formation of disulfide bridges implied the generation of Cu(I) by the peptide in a redox reaction. We used the Cu(I) indicator and chelator bathocuproine disulfonic acid (BCS) in a colorimetric assay to visualize Cu(I) production. The complex of BCS together with Cu(I) has an absorption maximum at 480 nm . BCS and Cu(II) were preincubated, and a scan from 390 to 590 nm was recorded during a stepwise addition of $1\text{ }\mu\text{g}$ peptide aliquots (Figure 3a,b). The BACE1-TMS peptide was sufficient to reduce Cu(II) to Cu(I) as indicated by the increase of absorbance peaks at 480 nm (Figure 3a). Importantly, the BACE1-TMS variant C466A failed to generate a signal (Figure 3b).

To validate the involvement of Cu(I) by an independent approach, we provided Cu(I) by preincubating Cu(II) with ascorbic acid as a reducing agent to generate Cu(I). This led to the formation of predominantly trimeric peptide complexes at equimolar concentrations (Figure 3c lane two). It is essential to note that the variant peptide C466A did not form any oligomers upon incubation with Cu(I) (Figure 3d) indicating that the thiol groups are essential to coordinate Cu(I) in the trimeric complexes. Upon preincubation of Cu(II), ascorbic acid and a molar excess of BCS, the peptides only migrated as monomers. This finding is best explained by the assumption that all Cu(I) formed is chelated by BCS and that no Cu(I) is available for peptide–metal complex formation (Figure 3c,d). We conclude that Cu(I) is generated in a redox reaction from Cu(II) and that Cu(I) as well as the sulfhydryl group of Cys466 are essential components of trimeric peptide complexes.

To further assess the role of monovalent metal ions, we used Ag(I) which can be regarded as a redox-stable Cu(I) analogue.³⁷ Ag(I) formed trimeric complexes with the BACE1-TMS peptide similarly to Cu(I), but in addition, tetrameric assemblies were formed (Figure 3e). Ag ions were found in both trimeric and tetrameric complexes as shown by laser ablation ICP-MS (Figures 3h,i and S2). Of note, peptide dimers were not formed even at high concentrations of Ag(I) which is probably attributable to the lack of an Ag(I)-related oxidative potential. This result further implies that trimers might be stabilized by monovalent transition metal ions, either Cu(I) or Ag(I). The prominent tetrameric band was only observed with Ag(I), most likely due to a different complex

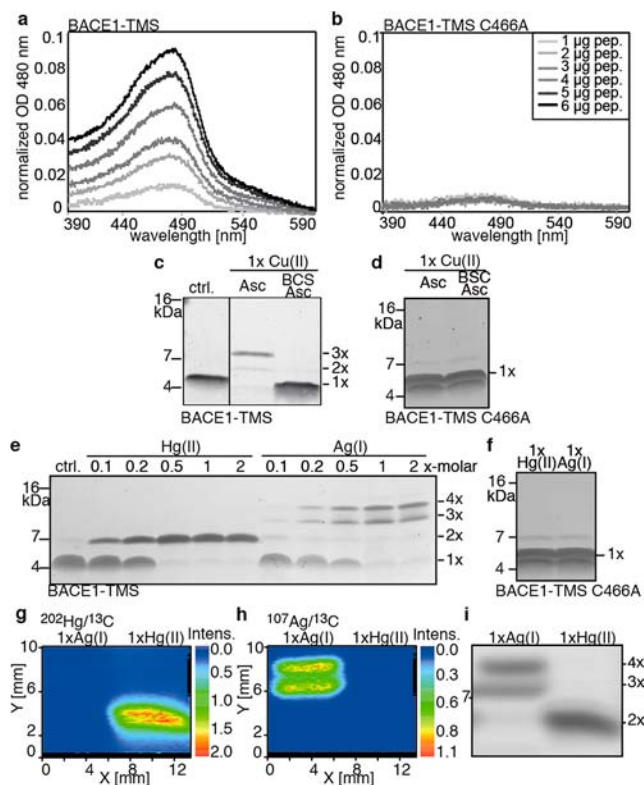


Figure 3. Involvement of monovalent transition-metal ions in oligomer formation. BCS colorimetric assay with (a) BACE1-TMS and (b) BACE1-TMS C466A, $n = 3$. (c) Preincubation of Cu(II) with ascorbic acid (Asc) reduces Cu(II) to Cu(I). BCS is a specific high-affinity Cu(I) chelator and preincubation of Cu(II) with both ascorbic acid and BCS only yields monomeric BACE1-TMS peptide (lane 3). (d) The peptide C466A does not form oligomers with Cu(I) generated by preincubation of Cu(II) with Asc. (e) Incubation of BACE1-TMS with Hg(II) and Ag(I) at indicated molar ratios. (f) Peptide C466A with Hg(II) or Ag(I). Laser ablation ICP-MS showing (g) $^{202}\text{Hg}/^{13}\text{C}$ and (h) $^{107}\text{Ag}/^{13}\text{C}$ signals of gels loaded with peptide BACE1-TMS and equimolar Ag(I) or Hg(II) depicted as heat map images. (i) Coomassie brilliant blue stained control gel. Gels shown in panels c–f are representative gels of at least three independent experiments, nonreducing conditions, silver stained.

geometry since the ionic radius of Ag(I) is larger compared to Cu(I).

As a further prove of the Cys466-mediated dimerization, we used Hg(II). Hg(II) is known to form linear, mercuric conjugates with free thiol groups of cysteine residues when the estimated distance for two sulfhydryls is in the range of 4–5 Å.³⁸ The treatment with Hg(II) was efficient in cross-linking BACE1-TMS peptides exclusively to dimers for the lowest molar ratios of peptide:Hg(II) onward (Figure 3e). As expected, mercury was detected in the Hg(II)-induced peptide dimers by laser ablation ICP-MS (Figures 3g,i and S2). Again, the variant peptide C466A did not form complexes with Ag(I) or Hg(II) (Figure 3f). Other transition-metal ions like zinc(II), cobalt(II), manganese(II) and nickel(II) were unable to mediate dimer formation (Figure S2). Collectively, trimerization of the peptide BACE1-TMS requires monovalent transition-metal ions and the sulfhydryl group of Cys466.

Met462 and Met470 in Oligomerization. Since Met-rich sequences are known to bind Ag(I) and Cu(I), we tested whether M462A and M470A variant peptides allow BACE1-TMS peptide oligomerization with Cu(II) (Figure 4). BACE1-TMS M462A formed predominantly trimers, but also dimers and tetramers upon Cu(II) addition. Excess Cu(II) led only to dimer formation (Figure 4a). Overall, the oligomerization behavior of the variant M462A closely resembles the BACE1-TMS peptide (compare Figures 1b and 4a). The variant peptide M470A predominantly formed tetramers in addition to trimers and dimers in the presence of (sub)-equimolar Cu(II) concentrations (Figure 4b). Therefore, the peptide M470A differs from the BACE1-TMS peptide and resembles more the BACE1-TMS-Ag(I) complexes in its coordination behavior. The lack of Met470 may change the metal ion coordination sphere in a way that four peptide molecules are required to complex Cu(I) under these conditions. Importantly, both peptides M462A and M470A produced Cu(I) to a similar extent as the BACE1-TMS peptide as indicated by the BCS-Cu(I) colorimetric assay results (Figure 4c,d). Also, both variant peptides M462A and M470A show a predominant α -helical conformation in 80% MetOH similar to the BACE1-TMS peptide, which is maintained at equimolar concentrations of Cu(II) added (Figure 4e,f). Taken together, Cys466 and Met470 are the major amino acids of the BACE1-TMS peptide to coordinate Cu(I).

Molecular Modeling. Tertiary structure models of BACE1-TMS trimers were built applying Rhythm, a tool that predicts TMS contact sites from sequence patterns and conservation

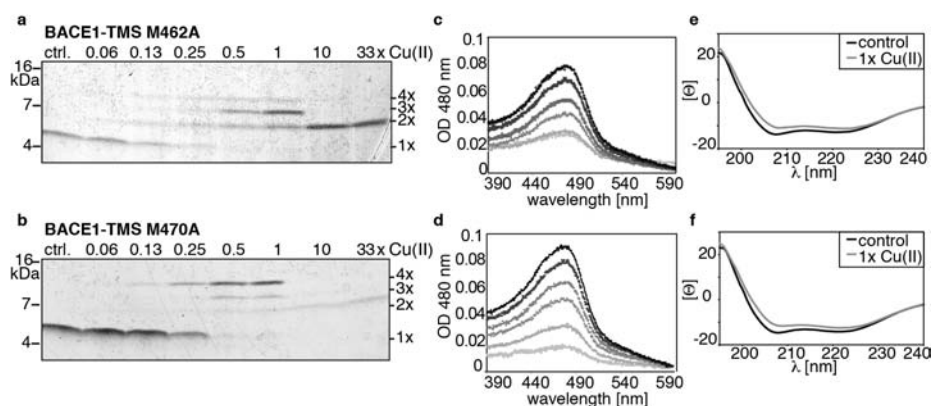


Figure 4. Methionine residues in metal binding. (a, c, e) BACE1-TMS M462A. (b, d, f) BACE1-TMS M470A. (a, b) Cu(II)-induced oligomer formation of variant peptides, nonreducing conditions, silver-stained SDS-PA gels, representative gel of three independent experiments. (c, d) BCS colorimetric assay. (e, f) CD spectroscopy.

criteria.³⁹ Analysis of the BACE1-TMS sequence reveals a recurrent octad repeat motif of buried and exposed residues (Figure 5a) and highlights Cys466 and Met470 as central

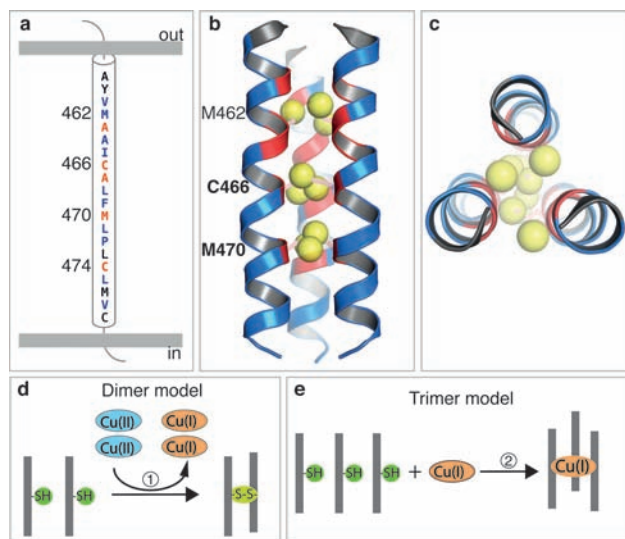


Figure 5. Tertiary structure model of the BACE1-TMS trimer. (a) Tertiary structure contacts of the wild-type BACE1-TMS predicted to be buried within the oligomer (red) or exposed to the membrane (blue) using Rhythm. All helical tertiary structure models of the BACE1-TMS reveal a sulfur-rich core (sulfur atoms as translucent yellow balls) of the BACE1-TMS (b) side-view (bold: key residues) or (c) top view of the trimer; buried (red) or exposed (blue) residues. (d) Proposed reaction scheme. Cu(II) is reduced to Cu(I) yielding a Cys466-Cys466 disulfide bridge and thus peptide dimers. (e) At (sub)-equimolar concentrations, Cu(I) binds to remaining amounts of peptide monomers containing the reduced sulfhydryl group of Cys466 and coordinates peptide trimers.

residues of a TMS oligomerization motif. A symmetric assembly of BACE-TMS trimer is in excellent agreement with the predicted burial status of the residues (Figure 5b,c). BACE-TMS trimers form a sulfur-rich core flanked by hydrophobic residues. Close interactions of Cys466 and Met470 in the N-terminal halves of the BACE-TMSs are generally consistent with a role in disulfide bridge formation in the BACE-TMS dimer or monovalent transition-metal ion-induced oligomerization in the trimer.

DISCUSSION

A unique feature of BACE1 among other aspartic-acid proteases is the presence of a type I transmembrane sequence (Ile458 to Trp480 of BACE1). We describe herein the so far unrecognized MxxxCxxxM core sequence motif in the sulfur-rich BACE1 TMS. This core motif is identified as a novel Cu ion binding site that governs oligomerization through metal ion complexation.

We designed model peptides of the human BACE1-TMS, which enabled us to investigate metal ion binding and metal ion mediated oligomerization of the TMS uncoupled from the cytoplasmic and ectodomain of BACE1. We found that the peptide specifically forms trimers which are stabilized by Cu(I) ions applying a set of biophysical and colorimetric methods. Using Cys/Met to Ala substitution peptides, the amino acid residues Cys466 and Met470 were identified as key residues in metal ion–peptide complexes. Independent from the catalyzed redox reaction, Cys466 is essential for oligomerization since the

variant peptide C466A retained its monomeric state even with Ag(I) ions or when it was exposed to Cu(I) produced in *statu nascendi* through ascorbic acid. Sequence analysis and molecular modeling of the BACE1 TMS reveals that the sulfur-rich motif is part of a highly conserved helix–helix interaction motif and corroborates the key role of Cys466 for BACE1 trimerization.

Together, we propose the following reaction steps to occur upon incubating Cu(II) with the BACE1-TMS peptide. At equimolar concentrations of Cu(II) and peptide, disulfide-bonded peptide dimers are formed when Cu(II) is reduced to Cu(I) (Figure 5d). With the newly formed S–S bond, Cu(I) binding is prohibited, and it dissociates off. In a second step, released Cu(I) is bound by residual nonoxidized BACE1-TMS peptide trimers (Figure 5e). At excess Cu(II) concentrations, Cu(II) induces the formation of disulfide-bridged dimers, but because of the high concentrations, it either prevents trimer formation or displaces Cu(I) in the trimeric assemblies. The reaction only ends when all peptides are converted into disulfide-bridged dimers, which is evident from prevailing dimeric peptides in our experiments. Since trimers are formed under reducing conditions in the presence of ascorbic acid as well as with the redox-inactive Ag(I), and thus in the absence of disulfide-bridged dimers, trimers are rather formed by three monomers than by a disulfide-bridged dimer and one monomer, although the latter cannot be strictly excluded.

In the BACE1-TMS, Cys466 and Met470 are important residues for Cu(I)-binding/metal ion coordination. Selectivity of the BACE1 Cu(II)/(I)-site(s) may be determined by a specific coordination geometry favoring oligomerization of the peptide. Attempts to determine the affinity of the sulfur-rich BACE1 sequence by isothermal titration calorimetry failed, probably because too many enthalpic parameters were present, i.e., a redox reaction, binding, and oligomerization. However, we assume that the affinity of the BACE1-TMS Cu(I) site is rather low since Mx(x)Mx(x)M motifs bind Cu(I) with micromolar affinity classifying them as lower-affinity sites.^{40,41} In contrast, high affinity Cu(I) sites usually contain at least a double His motif. Since low binding affinities are typically applied by ion transporters and channels, one could consider a function of the BACE1 sequence in Cu(I) transport. In fact, formation of BACE1 trimers in the presence of Cu(I) ions resembles the trimer formation of the copper transport protein 1 (Ctr1).^{42–44} Ctr1 has a channel-like architecture, recruits Cu(I) via extracellular Met/His motifs, and then passes it to MxxxM motifs in the Ctr1 TMS before metal ions are transferred to cytosolic histidine/cysteine residues, and Cu(I) is acquired by one of the cytosolic Cu(I) chaperones.^{44,45} If BACE1 has a function in Cu-homeostasis, Cu(I) binding to the BACE1-TMS might affect substrate recognition and activity. Such potential effects are currently investigated by our laboratory.

METHODS

Alignment of BACE1 Orthologues. The sequences of the various BACE1 homologues were retrieved from the UniProtKB and aligned with the ClustalW2 algorithm (EMBL-EBI).

Peptide Design and Purification. The 31-residue peptide DESTLMTIAYVMAAICALFMLPLALMVAQWR was designed as BACE1-TMS. To increase the water solubility of the peptide, nine residues of the BACE1 sequence were added: eight to the N terminus and one to the C terminus. Residues Cys474 and Cys478 within the TMS of BACE1 (see Figure 1a) were substituted with Ala residues to avoid unwanted chemical reactions since C478 is not conserved in distant homologues and both Cys were previously reported to be

palmitoylated and therefore are probably inert for metal ion binding.⁴⁶ To identify metal coordinating amino acid residues, the peptides M462A (DESTLMTIAYVAAAICALFMLPLALMVAQWR), C466A (DESTLMTIAYVMAAIAALFMLPLALMVAQWR) and M470A (DESTLMTIAYVMAAICALFALPLALMVAQWR) were synthesized and purchased from PSL (Heidelberg), HPLC purified, except for C466A, which we purified in our lab (raw from PSL Heidelberg) by reverse phase chromatography. C466A peptides were dissolved in 60% acetonitrile (AcN)/0.1% trifluoroacetic acid (TFA) at 1.7 mg/mL, ultrasonicated, and centrifuged at 21 000 g to remove undissolved material. Aliquots of 50 μ L were injected onto a XBridge C4 column (3.5 μ m diameter, 4.6 \times 150 mm) Waters, Eschborn at a flow rate of 0.2 mL/min on a Hewlett-Packard Series 1100 with a thermostatted column compartment (Agilent 1200). A gradient from 60% AcN/0.1% TFA to 80% AcN/0.1% TFA over 30 mL and at 40 °C caused elution of the C466A peptide in the peak at fraction 10. The eluates of 13 repeated runs were pooled and vacuum dried. Integrity and purity of C466A peptides was verified by matrix-assisted laser-desorption/ionization-mass spectrometry (Figure S3).

Peptide Treatments and Gels. Peptides were dissolved in 80% methanol:20% H₂O, and aliquots were vacuum dried and peptide content determined by amino acid analysis (Genaxxon, Ulm) or by photometric analysis. The exact quantification of each aliquot was required for the exact peptide:metal ion ratio experiments. Samples were then redissolved for experiments in 80% methanol to a concentration of 0.2 μ g/ μ L. Stock solutions of 100 mM of CuCl₂, HgCl₂, NiCl₂, MnCl₂, and CoCl₂ were prepared in Milli-Q water. A ZnCl₂ solution of 200 mM was prepared in 0.01% acetic acid to avoid hydroxide formation, and AgNO₃ was dissolved in 50 mM ammonium acetate to a final concentration of 100 mM and further diluted in 80% methanol to achieve conditions amenable for individual experiments. Equimolar concentrations of peptides and metal ions (final peptide concentrations of 28.8 μ M) were incubated at room temperature for 10 min (longer incubation times caused the spontaneous formation of peptides dimers most likely by air oxygen) and vacuum dried to remove the methanol. Samples were solubilized in sample buffer and ultrasonicated before SDS-PAGE. For laser ablation ICP-MS, 7–10 μ g peptide solubilized in 70 μ L 80% methanol (plus 28.8 μ M Cu(II) where applicable) were used. For Cu(I) chelation, BCS was dissolved in 80% methanol and applied at 150 μ M final concentration. Peptide oligomers were visualized on 10–20% tris-tricine gels (Anamed, Darmstadt) by silver staining. Gentle conditions for electrophoresis of samples used for laser ablation ICP-MS were applied using 10–20 mA, 30 V overnight to avoid displacement of metal ions from peptide complexes during electrophoresis. Peptides were stained with Coomassie brilliant blue.

Colorimetric Assay for Cu(I) Detection. BCS (360 μ M final concentration) and CuCl₂ (20 μ M) were pre-incubated in 80% methanol, and then repeatedly 1 μ g of peptide was added to increase the molar peptide concentration by 720 nM by each addition. The absorbance spectrum was measured between 390 and 600 nm on a UV-vis spectrophotometer (Perkin-Elmer), and background was subtracted for each measurement. Finally ascorbic acid was added to reduce entire remaining Cu(II) to Cu(I) and to achieve maximum Cu(I)–BCS complex formation.

Laser Ablation ICP-MS. Laser ablation ICP-MS was performed using a LSX-213 Nd:YAG laser system (Cetac, Omaha, USA) coupled to an X-Series II Quadrupole ICP-MS (Thermo Fischer Scientific, Waltham, USA). The ablation cell is a prototype design from Prof. D. Günther (ETH Zürich) and a precursor to the one described by ref 47. It was altered by adding a second gas inlet opposite to the primary inlet. Before the analysis, the system was warmed up and tuned on a daily basis by ablating line scans with 200 μ m spot size, 10 μ m s⁻¹ scan rate, 20 Hz repetition rate, and 100% laser energy from a standard glass (NIST 612) while optimizing the parameters for high signal intensities, low oxides, and a 238U/232Th ratio close to 1. Water was extracted from gels for laser ablation experiments by three to four incubations in 100% glycerol for 10 min each. The gels were cut according to the interested protein areas and attached to microscopic slides. After drying at room temperature for two days, the slides were

fixed in the ablation cell, which mechanically moves the gel piece in *xyz*-direction under the fixed laser. The samples were ablated by the laser at a scan rate of 50 μ m s⁻¹, spot size 200 μ m, repetition rate 20 Hz, laser energy \sim 1.2 mJ, and lane distance 100 μ m generating the aerosol. The particles were transported by a He carrier gas flow (0.9 l min⁻¹) from the cell to the ICP-MS, where an additional Ar gas flow (0.5 l min⁻¹) was introduced prior to the atomization and ionization in the plasma. Under the applied laser ablation parameters, the gels were not completely ablated, but lines of fairly constant diameter (50 μ m) and depth were removed and analyzed. For imaging a gel area, parallel, adjacent line scans were ablated, and the resulting time-dependent ICP-MS scans for each line merged to one data set using Origin software (OriginLab, version 8.6 0G.).

CD Spectroscopy. For CD spectroscopy, samples containing 140 μ M peptide in 80% methanol were measured on a Jasco J-810 spectropolarimeter at a path length of 1 mm at 20.0 °C, using 100 nm/min scanning speed, 1 s response time, and three scans per measurement. Buffer control was subtracted from each sample spectrum. Cu(II) was added at equimolar concentrations.

FT-IR. Measurements were carried out on an IFS 66v/S FT-IR spectrometer (Bruker Optics, Rheinstetten, Germany) equipped with a liquid nitrogen cooled mercury cadmium telluride (MCT) detector.⁴⁸ Spectral resolution was set to 4 cm⁻¹, and 1024 spectra were averaged for each measurement. The Blackman-Harris-3-Term apodization function was used prior to Fourier transformation. Aliquots of 10 μ L of a 10 mg/mL solution of the BACE1-TMS peptide in 80% methanol were attached by hydrophobic interactions to the surface of a silicon ATR cell (three active reflections, RESULTEC analytic equipment, Illerkirchberg, Germany) by drying with a gentle stream of air for a few minutes. The resulting thin film was rehydrated with 40 μ L water, and the FT-IR absorption spectrum was recorded after full equilibration of the sample. For the induction and measurements of FT-IR difference spectra, the water was exchanged by 50 μ L of 20 mM CuCl₂ in water (34-fold molar excess of Cu(II) with respect to the peptide). When the spectral changes reached saturation, the addition of the copper-containing buffer was repeated. The resulting difference spectrum was baseline corrected with the help of the OPUS software.

Raman Spectroscopy. Spectra were measured on a LABRAM spectrometer (Jobin Yvon, Bensheim, Germany) with the 568 nm line emitted by a krypton ion laser (Innova 90C, Coherent, Dieburg, Germany).⁴⁹ The laser beam with a power of 25 mW was focused onto the sample to a spot size of about 0.5 mm using a microscope (Olympus). The integration time of the charged coupled device (CCD) detector was set to result in a maximal signal of \sim 85% of the dynamic range of the detector. For each spectrum, 200 spectral recordings were averaged. The sample containing BACE1-TMS peptide was fixed onto a glass slide by air drying a 5 μ L drop of a 10 mg/mL peptide solution in 80% methanol. To thicken the peptide film (of finally \sim 500 μ m), the procedure was repeated five times and involved a total of 2 mg peptide. This peptide film was rehydrated with 20 μ L water for measurement. The peptide film was redissolved in 30 μ L 80% methanol, 142 mM CuCl₂ was added (50-fold molar excess of Cu(II) with respect to the peptide) and incubated for 20 min, and the peptide was again stepwise air dried on a glass slide. The recorded Raman spectra were corrected for the background fluorescence using the LabSpec 5 software.

Molecular Modeling. The hypothetical model of the wild-type BACE1 TMS trimer was built based on the tertiary structure contacts predicted by Rhythm.³⁹ Rhythm provides two different matrices for tertiary contact predictions of TMS. The first matrix is characteristic for right-handed ('channels'), the second for left-handed or parallel TMS packing interactions ('coils'). It is striking that octad-repeat patterns of buried and exposed residues are identified with both matrices (preset: medium specificity). The predicted octad-repeat patterns of buried and exposed residues indeed either matches with a right-handed packing arrangement of a BACE1 TMS dimer or a parallel arrangement of a trimer. For model building, we presumed an ideal α -helical conformation and a symmetric arrangement of the BACE1 TMS trimer. The interhelical crossing angles were then shifted until the predicted, and the actual burial status of each residue

matched.³⁹ The BACE1 TMS trimer model was finally subject of an energy minimization protocol performed in vacuum.⁵⁰

■ ASSOCIATED CONTENT

📄 Supporting Information

Figures S1–S3. This material is available free of charge via the Internet at <http://pubs.acs.org>.

■ AUTHOR INFORMATION

Corresponding Author

gerhard.multhaup@mcgill.ca

Present Addresses

^VT.B.: Transplantation and Clinical Virology, Department of Biomedicine – Haus Petersplatz, University of Basel, CH-4003 Basel, Switzerland

[#]F.L.: Integrated Program in Neuroscience, McGill University, Montreal, Canada

[○]M.S.: Max Planck Institute for Polymer Research, Department of Molecular Spectroscopy, Ackermannweg 10, 55128 Mainz, Germany

Notes

The authors declare no competing financial interest.

■ ACKNOWLEDGMENTS

We thank Prof. Koksche, Department of Biology, Chemistry and Pharmacy, Freie Universität Berlin for help with CD measurements and Dr. Magnus Mayer for technical support. This work was funded by the Deutsche Forschungsgemeinschaft (DFG) through MU901 and HI 1502, the Sonderforschungsbereich SFB740 (to G.M. and P.W.H.) and the International Copper Association (ICA).

■ REFERENCES

- (1) Cao, L.; Rickenbacher, G. T.; Rodriguez, S.; Moulia, T. W.; Albers, M. W. *Sci. Rep.* **2012**, *2*, 231.
- (2) Hu, X.; Hicks, C. W.; He, W.; Wong, P.; Macklin, W. B.; Trapp, B. D.; Yan, R. *Nat. Neurosci.* **2006**, *9*, 1520–1525.
- (3) Rajapaksha, T. W.; Eimer, W. A.; Bozza, T. C.; Vassar, R. *Mol. Neurodegener.* **2011**, *6*, 88.
- (4) Willem, M.; Garratt, A. N.; Novak, B.; Citron, M.; Kaufmann, S.; Rittger, A.; DeStrooper, B.; Saftig, P.; Birchmeier, C.; Haass, C. *Science* **2006**, *314*, 664–666.
- (5) Yang, L. B.; Lindholm, K.; Yan, R.; Citron, M.; Xia, W.; Yang, X. L.; Beach, T.; Sue, L.; Wong, P.; Price, D.; Li, R.; Shen, Y. *Nat. Med.* **2003**, *9* (1), 3–4.
- (6) Vassar, R.; Bennett, B. D.; Babu-Khan, S.; Kahn, S.; Mendiaz, E. A.; Denis, P.; Teplow, D. B.; Ross, S.; Amarante, P.; Loeloff, R.; Luo, Y.; Fisher, S.; Fuller, J.; Edenson, S.; Lile, J.; Jarosinski, M. A.; Biere, A. L.; Curran, E.; Burgess, T.; Louis, J. C.; Collins, F.; Treanor, J.; Rogers, G.; Citron, M. *Science* **1999**, *286*, 735–741.
- (7) Citron, M.; Oltersdorf, T.; Haass, C.; McConlogue, L.; Hung, A. Y.; Seubert, P.; Vigo-Pelfrey, C.; Lieberburg, I.; Selkoe, D. J. *Nature* **1992**, *360*, 672–674.
- (8) Jonsson, T.; Atwal, J. K.; Steinberg, S.; Snaedal, J.; Jonsson, P. V.; Bjornsson, S.; Stefansson, H.; Sulem, P.; Gudbjartsson, D.; Maloney, J.; Hoyte, K.; Gustafson, A.; Liu, Y.; Lu, Y.; Bhangale, T.; Graham, R. R.; Huttenlocher, J.; Bjornsdottir, G.; Andreassen, O. A.; Jonsson, E. G.; Palotie, A.; Behrens, T. W.; Magnusson, O. T.; Kong, A.; Thorsteinsdottir, U.; Watts, R. J.; Stefansson, K. *Nature* **2012**, *488*, 96–99.
- (9) Jin, S.; Agerman, K.; Kolmodin, K.; Gustafsson, E.; Dahlqvist, C.; Jureus, A.; Liu, G.; Falting, J.; Berg, S.; Lundkvist, J.; Lendahl, U. *Biochem. Biophys. Res. Commun.* **2010**, *393*, 21–27.
- (10) Schmechel, A.; Strauss, M.; Schlicksupp, A.; Pipkorn, R.; Haass, C.; Bayer, T. A.; Multhaup, G. *J. Biol. Chem.* **2004**, *279*, 39710–39717.

(11) Westmeyer, G. G.; Willem, M.; Lichtenthaler, S. F.; Lurman, G.; Multhaup, G.; Assfalg-Machleidt, I.; Reiss, K.; Saftig, P.; Haass, C. *J. Biol. Chem.* **2004**, *279*, 53205–53212.

(12) Yan, R.; Han, P.; Miao, H.; Greengard, P.; Xu, H. *J. Biol. Chem.* **2001**, *276*, 36788–36796.

(13) Benjannet, S.; Elagoz, A.; Wickham, L.; Mamarbachi, M.; Munzer, J. S.; Basak, A.; Lazure, C.; Cromlish, J. A.; Sisodia, S.; Checler, F.; Chretien, M.; Seidah, N. G. *J. Biol. Chem.* **2001**, *276*, 10879–10887.

(14) Kalvodova, L.; Kahya, N.; Schwille, P.; Ehehalt, R.; Verkade, P.; Drechsel, D.; Simons, K. *J. Biol. Chem.* **2005**, *280*, 36815–36823.

(15) Rajendran, L.; Schneider, A.; Schlechtingen, G.; Weidlich, S.; Ries, J.; Braxmeier, T.; Schwille, P.; Schulz, J. B.; Schroeder, C.; Simons, M.; Jennings, G.; Knolker, H. J.; Simons, K. *Science* **2008**, *320*, 520–523.

(16) Fukumoto, H.; Takahashi, H.; Tarui, N.; Matsui, J.; Tomita, T.; Hirode, M.; Sagayama, M.; Maeda, R.; Kawamoto, M.; Hirai, K.; Terauchi, J.; Sakura, Y.; Kakahana, M.; Kato, K.; Iwatsubo, T.; Miyamoto, M. *J. Neurosci.* **2010**, *30*, 11157–11166.

(17) Zhao, Y.; Wang, Y.; Hu, J.; Zhang, X.; Zhang, Y. W. *J. Biol. Chem.* **2012**, *287*, 11141–11150.

(18) Guo, Y.; Smith, K.; Lee, J.; Thiele, D. J.; Petris, M. J. *J. Biol. Chem.* **2004**, *279*, 17428–17433.

(19) Horng, Y. C.; Leary, S. C.; Cobine, P. A.; Young, F. B.; George, G. N.; Shoubridge, E. A.; Winge, D. R. *J. Biol. Chem.* **2005**, *280*, 34113–34122.

(20) Puig, S.; Lee, J.; Lau, M.; Thiele, D. J. *J. Biol. Chem.* **2002**, *277*, 26021–26030.

(21) Lutsenko, S. *Curr. Opin. Chem. Biol.* **2010**, *14*, 211–217.

(22) Bayer, T. A.; Schafer, S.; Simons, A.; Kemmling, A.; Kamer, T.; Tepest, R.; Eckert, A.; Schussel, K.; Eikenberg, O.; Sturchler-Pierrat, C.; Abramowski, D.; Staufienbiel, M.; Multhaup, G. *Proc. Natl. Acad. Sci. U.S.A.* **2003**, *100*, 14187–14192.

(23) Kessler, H.; Bayer, T. A.; Bach, D.; Schneider-Axmann, T.; Suppran, T.; Herrmann, W.; Haber, M.; Multhaup, G.; Falkai, P.; Pajonk, F. G. *J. Neural Transm.* **2008**, *115*, 1181–1187.

(24) Phinney, A. L.; Drisaldi, B.; Schmidt, S. D.; Lugowski, S.; Coronado, V.; Liang, Y.; Horne, P.; Yang, J.; Sekoulidis, J.; Coomaraswamy, J.; Chishti, M. A.; Cox, D. W.; Mathews, P. M.; Nixon, R. A.; Carlson, G. A.; St George-Hyslop, P.; Westaway, D. *Proc. Natl. Acad. Sci. U.S.A.* **2003**, *100*, 14193–14198.

(25) Singh, I.; Sagare, A. P.; Coma, M.; Perlmutter, D.; Gelein, R.; Bell, R. D.; Deane, R. J.; Zhong, E.; Parisi, M.; Ciszewski, J.; Kasper, R. T.; Deane, R. *Proc. Natl. Acad. Sci. U.S.A.* **2013**, *110*, 14771–14776.

(26) White, A. R.; Multhaup, G.; Galatis, D.; McKinstry, W. J.; Parker, M. W.; Pipkorn, R.; Beyreuther, K.; Masters, C. L.; Cappai, R. *J. Neurosci.* **2002**, *22*, 365–376.

(27) Bush, A. I.; Pettingell, W. H. J.; de Paradis, M.; Tanzi, R. E.; Wasco, W. *J. Biol. Chem.* **1994**, *269*, 26618–26621.

(28) Hesse, L.; Behr, D.; Masters, C. L.; Multhaup, G. *FEBS Lett.* **1994**, *349*, 109–116.

(29) Lovell, M. A.; Robertson, J. D.; Teesdale, W. J.; Campbell, J. L.; Markesbery, W. R. *J. Neurol. Sci.* **1998**, *158*, 47–52.

(30) Multhaup, G.; Schlicksupp, A.; Hesse, L.; Behr, D.; Ruppert, T.; Masters, C. L.; Beyreuther, K. *Science* **1996**, *271*, 1406–1409.

(31) Angeletti, B.; Waldron, K. J.; Freeman, K. B.; Bawagan, H.; Hussain, I.; Miller, C. C.; Lau, K. F.; Tennant, M. E.; Dennison, C.; Robinson, N. J.; Dingwall, C. *J. Biol. Chem.* **2005**, *280*, 17930–17937.

(32) Culotta, V. C.; Klomp, L. W.; Strain, J.; Casareno, R. L.; Krems, B.; Gitlin, J. D. *J. Biol. Chem.* **1997**, *272*, 23469–23472.

(33) Hildebrand, P. W.; Preissner, R.; Frommel, C. *FEBS Lett.* **2004**, *559*, 145–151.

(34) Barth, A. *Prog. Biophys. Mol. Biol.* **2000**, *74*, 141–173.

(35) Krimm, S.; Bandekar, J. *Adv. Protein Chem.* **1986**, *38*, 181–364.

(36) Van Wart, H. E.; Lewis, A.; Scheraga, H. A.; Saeva, F. D. *Proc. Natl. Acad. Sci. U.S.A.* **1973**, *70*, 2619–2623.

(37) Kittleson, J. T.; Loftin, I. R.; Hausrath, A. C.; Engelhardt, K. P.; Rensing, C.; McEvoy, M. M. *Biochemistry* **2006**, *45*, 11096–11102.

- (38) Soskine, M.; Steiner-Mordoch, S.; Schuldiner, S. *Proc. Natl. Acad. Sci. U.S.A.* **2002**, *99*, 12043–12048.
- (39) Rose, A.; Lorenzen, S.; Goede, A.; Gruening, B.; Hildebrand, P. *W. Nucleic Acids Res.* **2009**, *37*, W575–W580.
- (40) Jiang, J.; Nadas, I. A.; Kim, M. A.; Franz, K. J. *Inorg. Chem.* **2005**, *44*, 9787–9794.
- (41) Rubino, J. T.; Riggs-Gelasco, P.; Franz, K. J. *J. Biol. Inorg. Chem.* **2010**, *15*, 1033–1049.
- (42) Aller, S. G.; Eng, E. T.; De Feo, C. J.; Unger, V. M. *J. Biol. Chem.* **2004**, *279*, 53435–53441.
- (43) Haas, K. L.; Putterman, A. B.; White, D. R.; Thiele, D. J.; Franz, K. J. *J. Am. Chem. Soc.* **2011**, *133*, 4427–4437.
- (44) Lee, J.; Petris, M. J.; Thiele, D. J. *J. Biol. Chem.* **2002**, *277*, 40253–40259.
- (45) Cobine, P. A.; Ojeda, L. D.; Rigby, K. M.; Winge, D. R. *J. Biol. Chem.* **2004**, *279*, 14447–14455.
- (46) Vetrivel, K. S.; Meckler, X.; Chen, Y.; Nguyen, P. D.; Seidah, N. G.; Vassar, R.; Wong, P. C.; Fukata, M.; Kounnas, M. Z.; Thinakaran, G. *J. Biol. Chem.* **2009**, *284*, 3793–3803.
- (47) Fricker, M. B.; Kutscher, D.; Aeschlimann, B.; Frommer, J.; Dietiker, R.; Bettmer, J.; Günther, D. *Int. J. Mass Spectrom.* **2011**, *307*, 39–45.
- (48) Nyquist, R. M.; Ataka, K.; Heberle, J. *ChemBioChem* **2004**, *5*, 431–436.
- (49) Ataka, K.; Hegemann, P.; Heberle, J. *Biophys. J.* **2003**, *84*, 466–474.
- (50) Christen, M.; Hunenberger, P. H.; Bakowies, D.; Baron, R.; Burgi, R.; Geerke, D. P.; Heinz, T. N.; Kastenholz, M. A.; Krautler, V.; Oostenbrink, C.; Peter, C.; Trzesniak, D.; van Gunsteren, W. F. *J. Comput. Chem.* **2005**, *26*, 1719–1751.